# Barium spectrum in high magnetic fields

G. Droungas, N. E. Karapanagioti,* and J.-P. Connerade
*The Blackett Laboratory, Imperial College, London SW7 2BZ, United Kingdom*
(Received 15 July 1994)

We present the $l$- and $n$-mixing regions of the barium spectrum obtained in $\sigma$ polarization in a magnetic field of 2.89 T using one-step atomic-beam uv laser spectroscopy. Unexpected differences between the $\sigma^+$ and $\sigma^-$ spectra as well as extra structure are observed. An explanation in terms of the many-electron nature of the barium atom is proposed.

PACS number(s): 32.30.Jc, 32.60.+i

## I. INTRODUCTION

Recently, a number of studies of diamagnetic effects in atomic spectra have moved away from the pure diamagnetic problem and concentrated, instead, on nonhydrogenic systems, for which theoretical models now exist [1–4]. In particular, the case of He I [5] has attracted a lot of attention, being the next stage in complexity beyond hydrogen, and has been treated theoretically with great success [6].

The case of He, however, cannot bring out the full complexity of many-electron effects because the doubly excited configurations lie some 35 eV above the first ionization limit. Consequently, the high Rydberg spectra, while they are slightly disturbed by the non-Coulombic core, do not reveal any profound changes due to perturbations between excited states. In the alkaline earths, however, doubly excited states are found to straddle the ionization threshold, and appear as prominent perturbers of the principal series [7] even in the absence of external fields. There is, therefore, the new possibility of competition between correlations and the external field which renders these spectra very interesting. This is especially true of Ba I, which exhibits a remarkable perturbation of the principal series [8,9] resulting in a disappearance of oscillator strength around $n \sim 25$ followed by an increase in the higher members, due to an interaction with an autoionizing doubly excited resonance, labeled $5d8p\ ^1P_1$, which straddles the first ionization threshold.

It is precisely this circumstance, and the consequent ease of observing high Rydberg members in Ba I which led Garton and Tomkins [10] to perform the original study of diamagnetism in this spectrum. At the time, and in the subsequent early development of the theory of strong field atomic diamagnetism, the interpretation of this spectrum was performed within an independent electron scheme. It is now appropriate, in the light of more recent developments, to revisit this spectrum critically, in order to explore the interplay between the diamagnetic terms and electron-electron correlations. In the present paper, we describe experimental work on the spectrum of Ba I which has been performed with this general aim in mind.

## II. EXPERIMENTAL METHOD

The experimental setup is comprised of an effusive atomic beam propagating at right angles to the magnetic field provided by a dipole electromagnet, a left or right circularly polarized pulsed ultraviolet laser beam that propagates parallel to the magnetic field through a channel in the magnet poles, and a microchannel plate detector with its associated electronics that ionizes and detects highly excited atoms.

The atomic beam emerges from a resistive furnace, heated via high current copper feedthroughs inside a water-cooled stainless steel vacuum vessel. It is made of thin-walled (0.1 mm) stainless steel sheet, rolled and clamped into place with the sample inside, and a fine slit (0.1 mm wide) in the central section from which the diffusive beam can escape. It is heated by passing through it approximately 120 A of alternating current and the temperature is monitored with a thermocouple. The atomic beam is collimated using two apertures, the first being made of clamped and the second of externally adjustable jaws, so that the settings can be optimized from outside the vacuum system. In experiments so far, the collimation was such as to define a ratio of transverse to forward velocities of 1:270, yielding a Dopler width due to the transverse component of the order of 12 MHz, i.e., much smaller than the 2.4-GHz uv laser linewidth. At a temperature of 988 K, the barium beam moves at a mean velocity of 460 m/sec with a speed modified Maxwellian velocity distribution. Since (see below) the distance from the interaction region to the detector is 55 mm, the average time between excitation and detection is 120 $\mu$sec. This time delay is an important limitation of the measurements, as will be discussed below.

The atomic beam is led through an intermediate pumping chamber into the interaction chamber (see Fig. 1), between the poles of a large, conventional Zeeman magnet. This section has two ports for the atomic beam, plus one port set at a shallow angle for the detector, and two quartz windows on the sides for the ultraviolet laser

*Present address: Foundation for Research and Technology–Hellas Institute of Electronic Structure and Laser, 711 10 Heraklion, Crete, Greece.

 

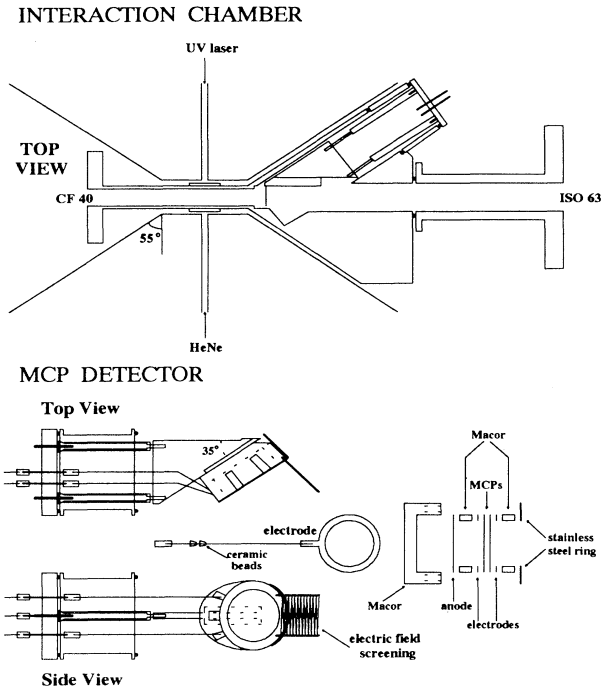


FIG. 1. Interaction chamber (top) and detail of microchannel plate detector (bottom).

beam, which thus crosses the path of the atomic beam and travels parallel to the magnetic field through the channel drilled in the pole pieces.

The detector is mounted in a side arm and as close as possible to the interaction region (see Fig. 1). It consists of two microchannel plates mounted in cascade to form a chevron and operated in the analog (nonsaturated) mode. The front plate is held at 800 V providing thus an electric field of 400 V/cm parallel to the magnetic field in the vicinity of the detector. Highly excited atoms emerging from the interaction region travel through 55 mm, pass through a shielding grid which protects the latter from electric field leakage, and are ionized by the electric field in front of the detector. The ensuing electrons are multiplied by the microchannel plates and the resulting signal is amplified, integrated, and digitized by the electronics. Microchannel plates were preferred to an electron multiplier or curved channeltron because they are much smaller and therefore more immune to the effects of fringe magnetic fields (of the order of 1–2 T in our experiments). They also operate very successfully in vacua of $10^{-5}$–$10^{-6}$ torr, whereas the superior (as far as magnetic field immunity is concerned) surface barrier detectors require an ultrahigh-vacuum environment [11]. However, information is lost due to effective loss of primary electrons (striking the inactive area of the plate) and due to the statistical variation in the gain (continuous as opposed to discrete multiplication). This results in a microchannel plate operated in the analog mode needing four times as many input electrons as a perfect multiplier with the same gain in order to provide the same information [12].

Another important limitation of the detection is the delay between excitation by the laser in the interaction volume and the moment when the excited atoms enter the detector. This time interval, as mentioned above, is about 120 $\mu$sec, and it follows that this method of detection favors long-lived atomic states. For high Rydberg states, this is not a problem in principle, but the faster a level decays (and the stronger the absorption line from the ground state to this level) the less it is likely to be detected by our method. Consequently, the sensitivity is biased towards an opposite class of excited states to those which are detected preferentially in photoabsorption. It is therefore of particular interest to compare our data with results obtained by photoabsorption spectroscopy.

The magnet is a large conventional dipole, capable of fields up to 3 T for a current of 500 A at 80 V, designed and built by Learner (unpublished). Its original purpose was the study of emission spectra, and it was therefore provided with a hole drilled right through the poles for the separation of $\pi$ from $\sigma$ spectra. In our experiment, we have used this channel for the laser beam, and therefore the atomic beam is perpendicular to the magnetic field. This arrangement maximizes the motional Stark effect and restricts its variance to that due to the distribution of atomic velocities (speed modified Maxwellian). Most experimental runs have been performed at flux densities $B=2.89\pm0.035$ T. The magnetic flux density is temporally stable to 1 part in 1000, and a homogeneity of better than 1% is achieved in the interaction region.

Both the excimer and dye lasers used for photoexcitation of the atomic beam are commercial units, manufactured by Lambdaphysik (EMG 201 MSC excimer laser with XeCl filling plus FL3002 dye laser operated in Coumarin 102), and the emerging beam was frequency doubled using a temperature-stabilized BBO crystal. For a pump energy of 300 mJ per pulse, the energy and linewidth of the uv output were 0.5 mJ and 2.4 GHz, respectively. To generate circularly polarized light from the linearly polarized laser beam, a Soleil-Babinet compensator is employed, made from natural quartz, and the circularity of the light is tested and checked between runs by reflecting the circularly polarized beam back through the compensator to be extinguished by a Glan-Taylor polarizer. This check was performed in darkness with adjusted eyesight and extinction was obtained for the middle of the wavelength range to be scanned and even for the longest scans of $\sim$0.3 nm remained satisfactory throughout the range. The intensity and wavelength of the laser beam were monitored during the experiments using a photodiode and an echelle grating spectrometer ($\pm$0.01 nm accuracy), respectively. Figure 2, which is a schematic representation of the experimental setup, shows all the components of the optical system. The prisms and lenses serve to transfer and collimate the uv beam quite a long way off to the electromagnet site.

The wavelength calibration was effected by taking magnetic field-free spectra $6s^2\,{}^1S_0 \rightarrow 6snp\,{}^1P_1$ and using the accurately known [13] (to five decimals in nm) Rydberg lines as wavelength markers. A small remanent magnetic field ($0.0165\pm0.0015$ T) and nonlinearities in the laser scans limited the wavelength accuracy to

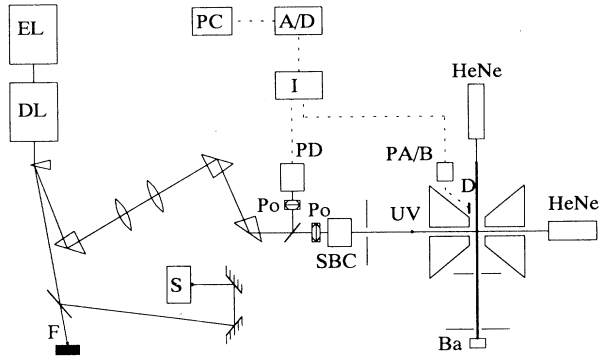


FIG. 2. Experimental setup: EL, excimer laser; DL, dye laser; *F*, fundamental; *S*, spectrometer; Po, polarizer; SBC, Soleil Babinet compensator; PD, photodiode; *D*, microchannel plate detector; PA/B, preamplifier/buffer; *I*, integrator.

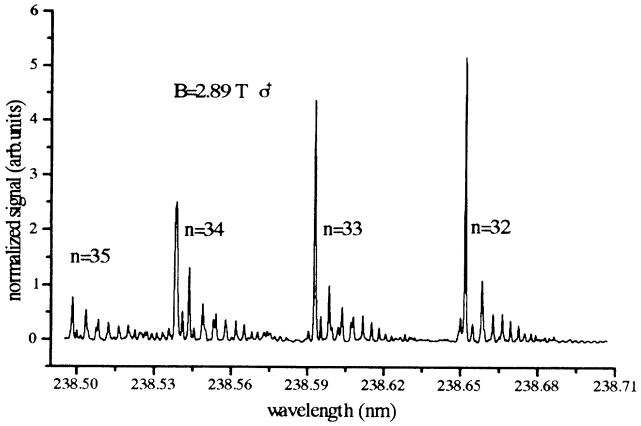


FIG. 3. Barium $M=+1$ odd total parity spectrum in the *l*-mixing region, obtained with one $\sigma^+$ polarized photon from the ground state in a magnetic field of 2.89 T.

$\pm 0.002$ nm. The SIMION computer code was used to check the electric field leakage from the detector into the interaction region. The electric field at the site where the laser and atomic beams meet was seen to be less than 0.003 V/cm. The 2.4-GHz laser bandwidth prevented us from obtaining an accurate estimate of the stray electric field present in the interaction region. A rather rough estimate was obtained from a *possible* shift of 0.000 04 nm (0.2 GHz) of the $6s^2\,{}^1S_0 \rightarrow 6s41p\,{}^1P_1$ magnetic field-free line when the ionizing voltage of the front microchannel plate was raised from 200 to 800 V. The scalar and tensor polarizabilities of the $6s^2\,{}^1S_0 \rightarrow 6s30d\,{}^1D_2$ line [14] were scaled ($n^{*7}$) to $n=41$ and an upper bound for the electric field of 2 V/cm was obtained.

## III. RESULTS

Σ-polarized spectra were obtained with the uv laser beam propagating parallel to the magnetic field of 2.89 T and inducing a one photon transition from the $6s^2\,{}^1S_0$ barium ground state to odd total parity, even *z*-parity states. The wavelength range examined (238.8–237.9 nm) covered the *l*- and *n*-mixing and quasi-Landau regions of the spectrum. Figures 3 and 4 show the *l*-mixing region obtained with left ($\sigma^+$) and right ($\sigma^-$) circularly polarized light, respectively. The $\sigma^+$ and $\sigma^-$ spectra were expected to be identical except for the paramagnetic shift. Garton, Tomkins, and Crosswhite [15] had stated explicitly in 1980 that "the $\sigma^+$ and $\sigma^-$ densitometer patterns superpose accurately, when relatively shifted by the appropriate Lorentz interval. This applies even to the detailed structure of the region around the zero-field limit." However, the spectra of Figs. 3 and 4 show significant differences between $\sigma^+$ and $\sigma^-$ and also have extra structure not recorded by Garton *et al.* The $\sigma^+$ spectrum has small secondary peaks between the *l*-mixed satellites, and the leading $K=1$ peak maintains its intensity. The $\sigma^-$ spectrum also has small peaks but these tend to be close to the satellites and thus are poorly resolved. A characteristic double peak is seen to lie higher in energy than the $K=1$ peak, the latter losing its intensity fast as *n* increases. Figure 5 shows the evolution of the $n=34$ $\sigma^-$ manifold with increasing magnetic field. It is seen in the figure that the $K=1$ leading line gradually loses its dominance as the magnetic field increases.

Figures 6, 7 and 8, 9 show the early and strong *n*-mixing regions, respectively, where again the $\sigma^+$ and $\sigma^-$ spectra differ appreciably. In addition the signal decreases rather drastically towards higher energies and no signal was obtained in the quasi-Landau region. Fairly constant intensity scales have been retained from spectrum to spectrum and thus the drop in intensity can be followed from Fig. 3 to 6 to 8 and from Fig. 4 to 7 to 9 for the $\sigma^+$ and $\sigma^-$ cases, respectively. Each spectrum has been obtained by linking together a small number (3–4) of wavelength portions taking care to keep the relative intensities intact. Although an effort has been directed to obtain good statistics, the information loss discussed above and possible saturation effects in the strongest peaks of each scan limit the trustworthiness of relative peak intensities, and some variations may occur.

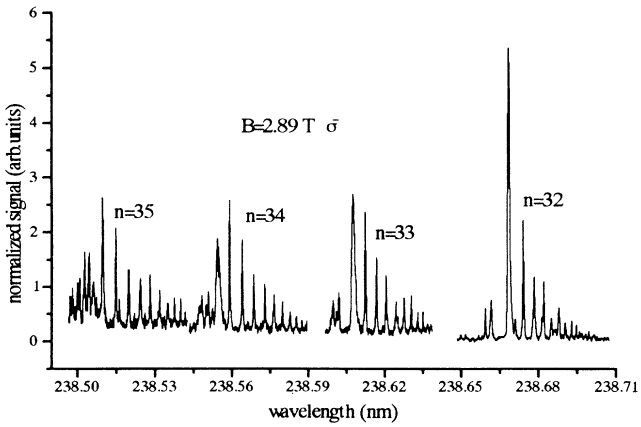


FIG. 4. Barium $M=-1$ odd total parity spectrum in the *l*-mixing region, obtained with one $\sigma^-$ polarized photon from the ground state in a magnetic field of 2.89 T.

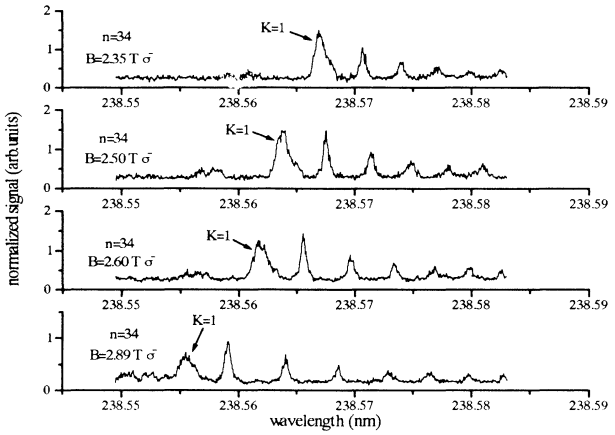


FIG. 5. Evolution of the $n=34$, $M=-1$ odd total parity barium manifold with increasing magnetic field.

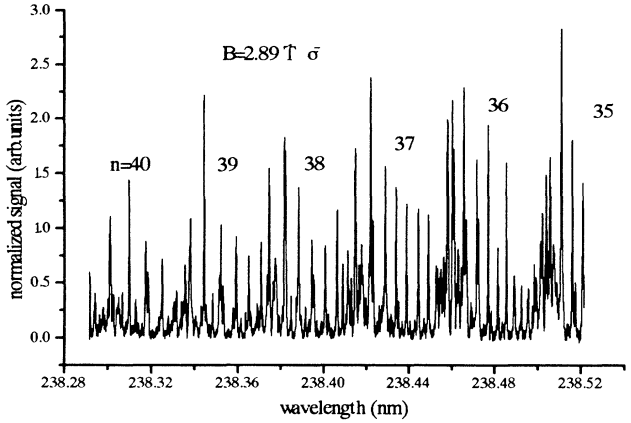


FIG. 7. Barium $M=-1$ odd total parity spectrum in the early $n$-mixing region, obtained with one $\sigma^-$ polarized photon from the ground state in a magnetic field of 2.89 T.

## IV. DISCUSSION

The observed differences between the $\sigma^+$ and $\sigma^-$ spectra and between our spectra and those of Garton, Tomkins, and Crosswhite [15] and rather intriguing. A possible explanation for the extra structure could arise by considering the effect of a small electric field on the spectrum. First let us consider parallel electric and magnetic fields. This case could arise from spurious fields, such as could leak into the interaction region from the electric field ionization region. An electric field parallel to the magnetic field would induce parity mixing as the total parity would not be strictly conserved and extra peaks would appear in the spectrum; the system has cylindrical symmetry, $L_z$ is conserved, and $M$ is a good quantum number. However, the experiments of Cacciani *et al.* [16] on lithium in parallel magnetic and electric fields have shown that for the odd total parity, $M=\pm 1$, $n=30$ manifolds in $B=2.33$ T the extra structure, that relates to the even components of the pure diamagnetic spectrum, appears for electric fields of the order of 75 V/cm. As discussed above, the spurious electric fields are less than 2 V/cm in our experiment and thus this explanation is unlikely.

On the other hand, we can consider the effect of the motional electric field ($|\mathbf{E}|=|\mathbf{v}\times\mathbf{B}|=vB\sin\alpha$) which in our experimental setup is maximized as the atoms move at right angles to the magnetic field ($\mathbf{v}\perp\mathbf{B}, \alpha=90°$). For a mean atomic beam velocity of 460 m/sec ($T\sim 715\,°C$) an average motional electric field of 13 V/cm is obtained. For the experiments of Garton, Tomkins, and Crosswhite [15] and Lu *et al.* [17], that were performed in an absorption cell with atoms moving at all possible angles $\alpha$ with respect to the magnetic field, we can obtain an average value for the motional electric field by averaging the absolute value of $\sin\alpha$ for all possible angles $\alpha$ to obtain $\bar{E}=2\bar{v}B/\pi\sim 7$ V/cm for $B=2.5$ T and $T\sim 1000\,°C$. By comparison the analogous value in the lithium experiments of Lu *et al.* was 51 V/cm for $B=4.78$ T and

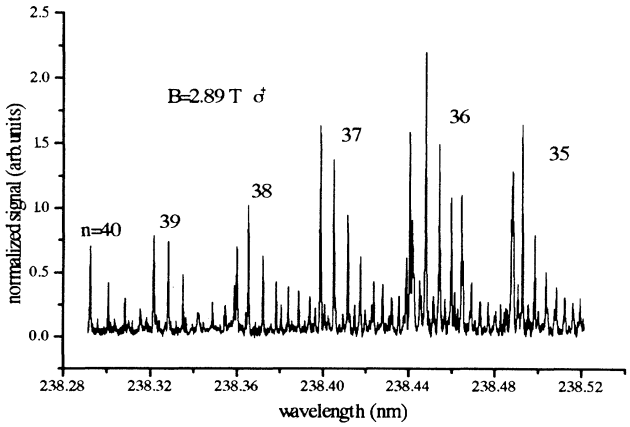


FIG. 6. Barium $M=+1$ odd total parity spectrum in the early $n$-mixing region, obtained with one $\sigma^+$ polarized photon from the ground state in a magnetic field of 2.89 T.

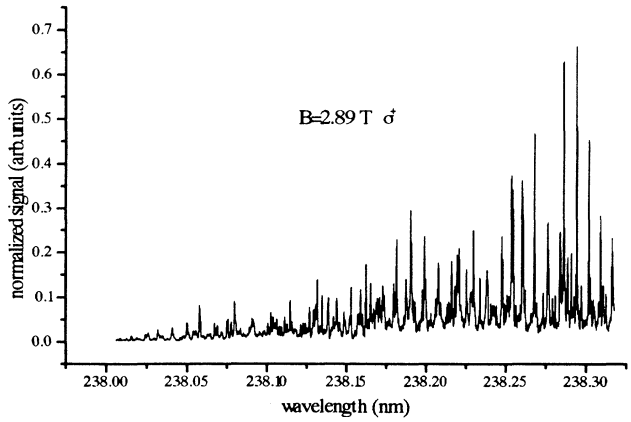


FIG. 8. Barium $M=+1$ odd total parity spectrum in the strong $n$-mixing region, obtained with one $\sigma^+$ polarized photon from the ground state in a magnetic field of 2.89 T.

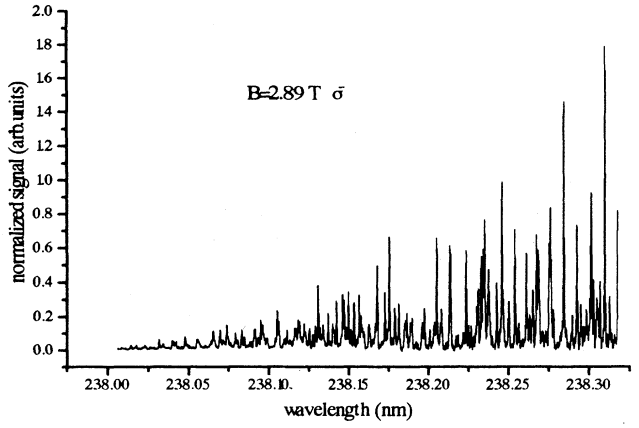


FIG. 9. Barium $M=-1$ odd total parity spectrum in the strong $n$-mixing region, obtained with one $\sigma^-$ polarized photon from the ground state in a magnetic field of 2.89 T.

$T=650\,^{\circ}\mathrm{C}$. This motional electric field has a direction normal to the magnetic field and thus destroys the cylindrical symmetry and strictly speaking neither parity nor $M$ are good quantum numbers. The extra structure observed in the lithium experiments arose due to $M$ mixing: Crosswhite *et al.* [18] calculated the relative transition probability of a "forbidden" ($\Delta M \neq \pm 1$) transition with respect to the allowed ($\Delta M = \pm 1$) transition. For lithium at $n=21$ and the fields and speed stated above this probability turns out to be 0.1. A similar calculation for our conditions with barium at $n=33$ results in a relative probability of 0.01. This rough estimate indicates that the heights of the extra peaks that would appear due to the motional electric field would be approximately two orders of magnitude smaller than that of the leading line of the pure diamagnetic manifold. This is not in accordance with the spectra shown in Figs. 3 and 4 and thus the motional electric field explanation also seems unlikely.

Considering now the differences between the $\sigma^+$ and $\sigma^-$ spectra obtained in our experiment we need to note that, as far as we are aware, the only other case where the $\sigma^+$ and $\sigma^-$ spectra have been reported as different was in the experiments of Garton *et al.* [19] on indium where the large spin-orbit term of the final $D$ state was of the order of the paramagnetic one for $n \approx 20$ and $B=4$ T. This results in a case intermediate between Zeeman and Paschen Back and in the inclusion of a *quadratic Zeeman* term in the Hamiltonian to describe the nonparallelism of the total magnetic moment to the total angular momentum in the strong magnetic field. Thus the two terms quadratic in the magnetic field, namely, the quadratic Zeeman and the diamagnetic, coexist and result in the $\sigma^+$ and $\sigma^-$ spectra differing substantially.

In the case where the transition of interest is singlet to singlet ($S=0$) the distinction between Zeeman and Paschen Back does not apply. However, in barium, because the spin-orbit term is not so small with respect to the residual electrostatic term, $LS$ coupling does not hold rigorously and the $\Delta S=0$ rule is violated as manifested by the appearance of triplets in the magnetic field-free spectrum [7]. Now in barium there is configuration interaction between the principal $6snp\ ^1P_1$ series and the $5d8p\ ^1P_1$ doubly excited level that straddles the first ionization threshold ($^2S_{1/2}$) and gives the high $n$ members of the former series oscillator strength [8,9]. The interval ratio for $5d8p\ ^3P_{2,1,0}$ is $\sim 51$ as opposed to 2 (value for $LS$ coupling), indicating the strength of the spin-orbit term. Therefore the existence of the large spin-orbit term of the $5d8p$ doubly excited level in the presence of a strong magnetic field ($B \sim 3$ T) can lead to the coexistence of the quadratic Zeeman and diamagnetic terms, the latter being appreciable in the 1-mixing region of the $6snp$ series due to the large principal quantum number ($n \sim 30$). Thus, via configuration interaction, we can have the coexistence of the two quadratic terms and similarly to the indium case differences between the $\sigma^+$ and $\sigma^-$ spectra can occur.

We have access to the original data of Lu, Tomkins, and Garton [20] and, on close inspection, we have found differences between the $\sigma^+$ and $\sigma^-$ spectra rather similar to those reported here which had apparently escaped their attention. As reported elsewhere [21], we have investigated in some detail theoretically various terms in the Hamiltonian which could give rise to asymmetries of this kind. A possible cause for the differences arises purely from the many-body character of the barium atom. This leads to different matrix elements of the diamagnetic term for magnetic quantum numbers $M$ of different sign. These differences disappear in the one-electron case.

## V. CONCLUSION

We have obtained the odd total parity even $z$ -parity one-photon absorption spectrum of the barium atom in a magnetic field of 2.89 T, using atomic beam ultraviolet laser spectroscopy. Extra structure is found that cannot be accommodated by the existence of small spurious or motional electric fields. Differences between the $\sigma^+$ and $\sigma^-$ spectra are attributable to the many-electron character of the barium atom. Theoretical work is needed to investigate the competition of the spin-orbit and paramagnetic terms as well as the differences that arise when one treats the barium atom as a many-electron atom.

## ACKNOWLEDGMENTS

We would like to thank Brian Willey and Geoff Cox for their technical assistance, Xing Hong He for his help with the theory, and two of us (G.D. and N.E.K.) would like to thank the Republic of Greece for financial support via the State Scholarships Foundation.

[1] P. F. O'Mahony and K. T. Taylor, Phys. Rev. Lett. **57**, 2931 (1986).
[2] P. F. O'Mahony and F. Mota-Furtado, Phys. Rev. Lett. **67**, 2283 (1991).
[3] S. Watanabe and H. Komine, Phys. Rev. Lett. **67**, 3227 (1991).
[4] M. H. Halley, D. Delande, and K. T. Taylor, J. Phys. B **26**, 1775 (1993).
[5] T. van der Veldt, W. Vassen, and W. Hogervost, J. Phys. B **25**, 3295 (1992).
[6] D. Delande, K. T. Taylor, M. H. Halley, T. van der Veldt, W. Vassen, and W. Hogervost, J. Phys. B **27**, 2771 (1994).
[7] J. A. Armstrong, J. J. Wynne, and P. Esherick, J. Opt. Soc. Am. **69**, 211 (1978).
[8] W. R. S. Garton and K. Codling, Proc. Phys. Soc. London **75**, 87 (1960).
[9] J. P. Connerade and A. M. Lane, Rep. Prog. Phys. **51**, 1439 (1988).
[10] W. R. S. Garton and F. S. Tomkins, Astrophys. J. **158**, 839 (1969).
[11] P. Cacsciani, S. Liberman, E. Luc-Koenig, J. Pinard, and C. Thomas, J. Phys. B **21**, 3473 (1988).
[12] B. W. Manley, A. Guest, and R. T. Holmshaw, Adv. Electron. Electron Phys. **28A**, 471 (1969).
[13] W. R. S. Garton and F. S. Tomkins, Astrophys. J. **158**, 1219 (1969).
[14] K. A. H. van Leeuwen, W. Hogervost, and B. H. Post, Phys. Rev. A **28**, 1901 (1983).
[15] W. R. S. Garton, F. S. Tomkins, and H. M. Crosswhite, Proc. R. Soc. London, Ser. A **373**, 189 (1980).
[16] P. Cacciani, S. Liberman, E. Luc-Koenig, J. Pinard, and C. Thomas, J. Phys. B **21**, 3523 (1988).
[17] K. T. Lu, F. S. Tomkins, H. M. Crosswhite, and H. Crosswhite, Phys. Rev. Lett. **41**, 1034 (1978).
[18] H. Crosswhite, U. Fano, K. T. Lu, and A. R. P. Rau, Phys. Rev. Lett. **42**, 963 (1979).
[19] W. R. S. Garton, H. Crosswhite, H. M. Crosswhite, and F. S. Tomkins, Proc. R. Soc. London, Ser. A **400**, 55 (1985).
[20] K. T. Lu, F. S. Tomkins, and W. R. S. Garton, Proc. R. Soc. London, Ser. A **362**, 421 (1978).
[21] J.-P. Connerade, G. Droungas, R. Elliott, X. He, N. Karapanagioti, M. A. Farooq, H. Ma, J. P. Marangos, and M. Nawaz, J. Phys. B **27**, 2753 (1994).